Corrections to the Berry phase in a solid-state qubit due to low-frequency noise

Fernando C. Lombardo* and Paula I. Villar†

Departamento de Física Juan José Giambiagi, FCEyN UBA and IFIBA CONICET-UBA, Facultad de Ciencias Exactas y Naturales, Ciudad Universitaria, Pabellón I, 1428 Buenos Aires, Argentina

(Received 3 December 2013; published 15 January 2014)

We present a quantum open-system approach to analyze the nonunitary dynamics of a superconducting qubit when it evolves under the influence of external noise. We consider the presence of longitudinal and transverse environmental fluctuations affecting the system's dynamics and model these fluctuations by defining their correlation function in time. By using a Gaussian-like noise correlation, we can study low- and high-frequency noise contribution to decoherence and implement our results in the computation of geometric phases in open quantum systems. We numerically study when the accumulated phase of a solid-state qubit can still be found close to the unitary (Berry) one. Our results can be used to explain experimental measurements of the Berry phase under high-frequency fluctuations and design experimental future setups when manipulating superconducting qubits.

DOI: 10.1103/PhysRevA.89.012110 PACS number(s): 03.65.Vf, 03.65.Yz, 03.67.Lx, 05.40.Ca

I. INTRODUCTION

Geometric phases are closely linked to the classical concept of parallel transport of a vector on a curved surface. This analogy is particularly clear in the case of a two-level system (a qubit) in the presence of a biased field that changes in time. Take, for example, a spin-1/2 particle in a changing magnetic field. The general Hamiltonian for such a system is $H = \hbar/2\vec{R}\cdot\vec{\sigma}$, where $\vec{\sigma} = (\sigma_x,\sigma_y,\sigma_z)$ are the Pauli operators and $\vec{R}$ is the biased field vector. The qubit state can be represented by a point on a sphere of unit radius, called a Bloch sphere. This sphere can be embedded in a three-dimensional space of Cartesian coordinates, and hence the Bloch vector $\vec{R}$ is a vector whose components (x,y,z) single out a point on the sphere. This representation offers a particularly well-suited framework to visualize the dynamics of the qubit, which consists in the qubit state continually precessing about the vector $\vec{R}$, acquiring a dynamical phase $\gamma(t)$. If the evolution is done adiabatically, the qubit also acquires a geometric phase (GP), sometimes called a Berry phase.

It is known that the system can retain the information of its motion in the form of this GP, which was first put forward by Pancharatnam in optics [1] and later studied explicitly by Berry in a general quantal system [2]. Since then, great progress has been achieved in this field. The application of the GP has been proposed in many fields, such as the geometric quantum computation. Due to its global properties, the GP is propitious to construct fault-tolerant quantum gates. In this line of work, many physical systems have been investigated to realize geometric quantum computation, such as NMR [3], Josephson junctions [4], ion traps [5], and semiconductor quantum dots [6]. The quantum computation scheme for the GP has been proposed based on the Abelian or non-Abelian geometric concepts, and the GP has been shown to be robust against faults in the presence of some kind of external noise due to the geometric nature of the Berry phase [7–9]. Then, for isolated quantum systems, the GP is theoretically perfectly understood and experimentally verified. However, it was seen that the interactions play an important role in the realization of some specific operations. As the gates operate slowly compared to the dynamical time scale, they become vulnerable to open-system effects and parameter fluctuations that may lead to a loss of coherence. Consequently, study of the GP was soon extended to open quantum systems. Following this idea, many authors have analyzed the correction to the GP under the influence of external thermal or nonequilibrium environments using different approaches (see [10–15] and references therein). In all cases, the purely dephasing model considered was a spin-1/2 particle coupled to the environment's degrees of freedom through a σ_z coupling. Interest in the GP in open systems has also been extended to some experimental setups [16].

The GP is a promising building block for noise-resilient quantum operations. Lately, the GP has also been observed in a variety of superconducting systems [17,18]. Superconducting circuits are good candidates to potentially manipulate quantum information efficiently. Current circuit technology allows scaling to large and more complex circuits [19,20]. Several experiments with superconducting Josephson-junction circuits have demonstrated quantum coherent oscillations with a long decay time, probing coherent properties of Josephson qubits and positioning them as useful candidates for applications in quantum computing and quantum communication. Despite the long coherence times of the quantum state, the decoherence-induced process still deserves study for using these circuits for the development of a quantum processor. When the two lowest energy levels of a current-biased Josephson junction are used as a qubit, the qubit state can be fully manipulated with low- and microwave-frequency control currents. Circuits presently being explored combine in variable ratios the Josephson effect and single Cooper-pair charging effects. In all cases the Hamiltonian of the system can be written

$$H = \frac{\hbar}{2}\omega_a\sigma_z + \hbar\Omega_{\rm R}\cos(\omega t + \varphi_{\rm R})\sigma_x, \qquad (1)$$

where $\hbar\Omega_{\rm R}$ is the dipole interaction amplitude between the qubit and the microwave field of frequency ω and phase $\varphi_{\rm R}$. $\Omega_{\rm R}/2\pi$ is the Rabi frequency. This Hamiltonian can

*lombardo@df.uba.ar
†paula@df.uba.ar

be transformed to a rotating frame at the frequency ω by means of a unitary transformation, resulting in a new effective Hamiltonian of the form

$$H_{\rm eff} = \frac{\hbar}{2}(\Delta\sigma_z + \Omega_x\sigma_x + \Omega_y\sigma_y), \tag{2}$$

where $\Omega_x = \Omega_{\rm R}\cos\varphi_{\rm R}$ and $\Omega_y = \Omega_{\rm R}\sin\varphi_{\rm R}$. This model is similar to the generic situation of a qubit in a changing magnetic field, where $\mathbf{R} = (\Omega_x, \Omega_y, \Delta)$ and $\Delta = \omega_a - \omega$ is the detuning between the qubit transition frequency and the applied microwave frequency. In an experimental situation [18] Δ can be kept fixed and one can control the biased field to trace circular paths of different radii $\Omega_{\rm R}$.

The same physical structures that make these superconducting qubits easy to manipulate, measure, and scale are also responsible for coupling the qubit to other electromagnetic degrees of freedom that can be a source of decoherence via noise and dissipation. Thus a detailed mechanism of decoherence and noise due to the coupling of Josephson devices to external noise sources is still required. It has been shown that low-frequency noise is an important source of decoherence for superconducting qubits. Generally, this noise is described by fluctuations in the effective magnetic field which are directed either in the z axis, longitudinal noise, or in a transverse direction, transversal noise. Both types of noise have been phenomenologically modeled by making different assumptions on these fluctuations, such as being due to a stationary, Gaussian and Markovian process [17]. Others, have considered that the $1/f$ noise must be rooted in a non-Gaussian long-time correlation stochastic process. In the context of quantum information, the implication of long-time correlations of stochastic processes is that the effects suffered by the system's evolution due to the $1/f$ noise are protocol or measurement dependent. Apparently, some protocols clearly reveal a non-Gaussian nature while others Gaussian approximations attain the main effects in a short-time scale [21].

In this manuscript, we shall present a fully quantum open-system approach to analyze the nonunitary dynamics of the solid-state qubit when it is considered evolving under the influence of external fluctuations. We consider the qubit coupled in longitudinal and transversal directions. As a physical example, we study the dynamics and decoherence-induced process on the superconducting qubit. We further analyze when the accumulated phase gained by the system after one period can still be found close to the unitary (Berry) phase and focus on the importance of the longitudinal coupling as a source of decoherence. The paper is organized as follows: In Sec. II, we develop a general quantum open-system model in order to consider different types of fluctuations (longitudinal and/or transverse) that induce decoherence on the main system. By means of a general master equation for the reduced density matrix of the qubit, we follow the nonunitary evolution characterized by fluctuations, dissipation, and decoherence. This gives us complete insight into the state of the system: complete knowledge of different dynamical time scales and analysis of the effective role of noise sources inducing decoherence. Section III contains the numerical evaluation of the geometric phase and its noise-induced corrections for the several scenarios considered. We shall emphasize the effect of longitudinal and transversal noise on the global geometric phase. Comparison between theory and experiment verifies our understanding of the physics underlying the system as a dissipative two-level device. Berry's-phase measurements provide an important constraint to take into account with regard to noise models and their correction induced over the GP, at least at the times in which the experiments are performed. Comprehension of the decoherence and dissipative processes should allow their further suppression in future qubits designs or experimental setups. In Sec. IV we summarize our findings.

II. MASTER EQUATION APPROACH TO DECOHERENCE IN A SUPERCONDUCTING QUBIT

We shall begin by deriving a general master equation for the reduced density matrix for the qubit (obtained after tracing out all the environmental degrees of freedom). The dynamics of a generic two-level system steered by a system's Hamiltonian of the type (where we have set $\hbar = 1$ all along the paper)

$$H_{\rm Total} = H_q + H_{\rm int} + H_{\mathcal{E}}, \text{ with} \tag{3}$$

$$H_q = \tfrac{1}{2}(\Omega\sigma_x + \Delta\sigma_z), \tag{4}$$

where we have defined a qubit Hamiltonian H_q similar to that of a solid-state qubit Eq. (2), setting $\varphi_{\rm R} = 0$ for simplicity, and $H_{\mathcal{E}}$ is the Hamiltonian of the bath. The interaction Hamiltonian is thought as some longitudinal and transverse noise coupled to the main system:

$$H_{\rm int} = \tfrac{1}{2}(\delta\hat{\omega}_1\sigma_x + \delta\hat{\omega}_0\sigma_z). \tag{5}$$

We must note that the system's unitary dynamics and coupling to the environment is different from the usual purely dephasing models proposed to study geometric phases in open systems (see Refs. [10–16]). We shall derive the master equation in the Born-Markov approximation for general noise terms $\delta\hat{\omega}_1$ and $\delta\hat{\omega}_0$ interacting with the system in the $\hat{x}$ and $\hat{z}$ directions, respectively. We will consider a weak coupling between the system and environment and that the bath is sufficiently large to stay in a stationary state. In other words, the total state ρ_{SE} (system and environment) can be split as

$$\rho_{SE} \approx \rho(t)\rho_{\mathcal{E}}, \tag{6}$$

for all times. It is important to stress that due to the Markov regime, we will restrict our discussions to cases for which the self-correlation functions generated at the environment (due to the coupling interaction) would decay faster than typical variation scales in the system. In this way, the evolution equation for $\rho(t)$ is local in time [22]. In the interaction picture, the evolution of the total state is ruled by the Liouville equation

$$\dot{\rho}_{SE} = -i[H_{\rm int}, \rho_{SE}], \tag{7}$$

where we have denoted the state ρ_{SE} in the interaction picture in the same way as before, just in order to simplify notation. A formal solution of the Liouville equation can be obtained

perturbatively using the Dyson expansion [23]:

$$\rho_{\mathcal{S}E}(t) = \sum_{n\geqslant 0}\int_0^t ds_1 \int_0^{s_1} ds_2 \ldots \int_0^{s_n} ds_n \left(\frac{1}{i}\right) \times[H_{\rm int}(s_1),[H_{\rm int}(s_2),[\ldots,[H_{\rm int}(s_n),\rho_{\mathcal{S}E}(0)]\ldots]]]. \tag{8}$$

From this expansion, one can obtain a perturbative master equation, up to second order, in the coupling constant between system and environment for the reduced density matrix $\rho = {\rm Tr}_{\mathcal{E}}\rho_{\mathcal{S}E}$. In the interaction picture the formal solution reads as

$$\rho(t) \approx \rho(0) - i\int_0^t ds {\rm Tr}_{\mathcal{E}}([H_{\rm int}(s),\rho_{\mathcal{S}E}(0)]) - \int_0^t ds_1 \int_0^{s_1} ds_2 {\rm Tr}_{\mathcal{E}}\{[H_{\rm int}(s),[H_{\rm int}(t),\rho_{\mathcal{S}E}(0)]]\}. \tag{9}$$

Taking the temporal derivative of the previous equation and assuming that system and bath are not correlated at the initial time, the master equation can be written as [22]

$$\dot\rho = -i\,{\rm Tr}_{\mathcal{E}}[H_{\rm int}(t),\rho(t)\rho_{\mathcal{E}}(0)] - \int_0^t ds\ {\rm Tr}_{\mathcal{E}}[H_{\rm int}(t),[H_{\rm int}(s),\rho(t)\rho_{\mathcal{E}}(0)]] + \int_0^t ds {\rm Tr}_{\mathcal{E}}\{[H_{\rm int}(t),{\rm Tr}_{\mathcal{E}}[H_{\rm int}(s),\rho(t)\rho_{\mathcal{E}}(0)]\rho_{\mathcal{E}}(0)]\}.$$

Considering that the $\delta\hat\omega_i$ of the $H_{\rm int}$ [Eq. (5)] are operators acting only on the Hilbert space of the environment (and the Pauli matrices applied on the system Hilbert space), the master equation, in the Schrödinger picture, can be written as

$$\dot\rho = -\int_0^t ds\ {\rm Tr}_{\mathcal{E}}[H_{\rm int}(t),[H_{\rm int}(s),\rho(t)\rho_{\mathcal{E}}(0)]]. \tag{10}$$

The master equation explicitly reads

$$\dot\rho = -i[H_q,\rho] - D_{xx}(t)[\sigma_x,[\sigma_x,\rho]] - f_{xy}(t)[\sigma_x,[\sigma_y,\rho]] - f_{xz}(t)[\sigma_x,[\sigma_z,\rho]] - f_{zx}(t)[\sigma_z,[\sigma_x,\rho]] - f_{zy}(t)[\sigma_z,[\sigma_y,\rho]] - D_{zz}(t)[\sigma_z,[\sigma_z,\rho]], \tag{11}$$

where the noise coefficients are given by

$$\begin{aligned} D_{xx}(t) &= \int_0^t ds\ \langle\delta\hat\omega_1(0)\delta\hat\omega_1(-s)\rangle_{\mathcal{E}}\ X_1(-s),\\ f_{xy}(t) &= \int_0^t ds\ \langle\delta\hat\omega_1(0)\delta\hat\omega_1(-s)\rangle_{\mathcal{E}}\ Y_1(-s),\\ f_{xz}(t) &= \int_0^t ds\ \langle\delta\hat\omega_1(0)\delta\hat\omega_1(-s)\rangle_{\mathcal{E}}\ Z_1(-s),\\ f_{zx}(t) &= \int_0^t ds\ \langle\delta\hat\omega_0(0)\delta\hat\omega_0(-s)\rangle_{\mathcal{E}}\ X_0(-s),\\ f_{zy}(t) &= \int_0^t ds\ \langle\delta\hat\omega_0(0)\delta\hat\omega_0(-s)\rangle_{\mathcal{E}}\ Y_0(-s),\\ D_{zz}(t) &= \int_0^t ds\ \langle\delta\hat\omega_0(0)\delta\hat\omega_0(-s)\rangle_{\mathcal{E}}\ Z_0(-s). \end{aligned} \tag{12}$$

It is possible to recognize D_{ab} and f_{ab} as normal and anomalous diffusion coefficients, respectively $(a,b = x,y,z)$. The functions $X_{0,1}, Y_{0,1}$, and $Z_{0,1}$ are derived by obtaining the temporal dependence of the Pauli operators σ_i in the Heisenberg representing through the differential equations,

$$\frac{d\sigma_k(t)}{dt} = i[H_q,\sigma_k(t)], \tag{13}$$

with $k = x,y,z$ and H_q as in Eq. (4). The solution can be expressed as a linear combination of the Pauli matrices (in the Schrödinger representation),

$$\sigma_z^{0,1} = X_{0,1}(t)\sigma_x + Y_{0,1}(t)\sigma_y + Z_{0,1}(t)\sigma_z. \tag{14}$$

The solution can be easily written as

$$\begin{aligned} X_1(t) &= \frac{\Omega^2+\Delta^2\cos(2t\sqrt{\Omega^2+\Delta^2})}{\Omega^2+\Delta^2},\\ Y_1(t) &= \frac{\Delta\sin(2t\sqrt{\Omega^2+\Delta^2})}{\sqrt{\Omega^2+\Delta^2}},\\ Z_1(t) = X_0(t) &= \frac{\Delta\Omega[1-\cos(2t\sqrt{\Omega^2+\Delta^2})]}{\Omega^2+\Delta^2},\\ Y_0(t) &= -\frac{\Omega\sin(2t\sqrt{\Omega^2+\Delta^2})}{\sqrt{\Omega^2+\Delta^2}},\\ Z_0(t) &= 1-\frac{\Omega^2[1-\cos(2t\sqrt{\Omega^2+\Delta^2})]}{\Omega^2+\Delta^2}. \end{aligned}$$

It is easy to check that if the Rabi frequency is zero and $\delta\hat\omega_1 = 0$, we recover the dynamics of a spin-1/2 precessing a bias field vector **R**.

The idea is to use different noise correlation functions to model different types of noise that can be found in solid-state qubits. Once the coefficients in Eq. (12) are defined, we can numerically solve the master equation and obtain the evolution in time of the reduced density matrix. Once this quantity is known, we can further obtain interesting features of the qubit dynamics such as the biased vector **R** and the decoherence induced on the superconducting qubit.

The noise correlations can be defined by their spectral density $J_i(\omega) = 1/(2\pi)\int dt e^{i\omega t}\langle\delta\hat\omega_i(0)\delta\hat\omega_i(-s)\rangle_{\mathcal{E}}$, with $i = 0,1$. Herein, we shall focus on the long- and short-correlated noise (slow and sharp decay of $\langle\delta\hat\omega_i(0)\delta\hat\omega_i(-s)\rangle$), i.e., on the noise power peaked at low or high frequencies. We will describe different types of noise as

$$\langle\delta\hat\omega_i(0)\delta\hat\omega_i(-s)\rangle_{\mathcal{E}} = \gamma_i\mathcal{F}(\alpha_i,t), \tag{15}$$

(where γ_i is a dissipative constant that includes the coupling strength between the system and bath, and α_i is a parameter with frequency units). This function $\mathcal{F}$ keeps the information about the correlation times and couplings in the environment. Phenomenologically, $\mathcal{F}$ can be thought as a Dirac δ functional for short correlations in the time domain, or a Gaussian-like function of time for a more general scenario. In solid-state systems decoherence is potentially strong due to numerous microscopic modes. Noise is dominated by material-dependent sources, such as background-charge fluctuations or variations of magnetic fields and critical currents, with a given power spectrum, often known as $1/f$. This noise is difficult to suppress and, since the dephasing is generally dominated

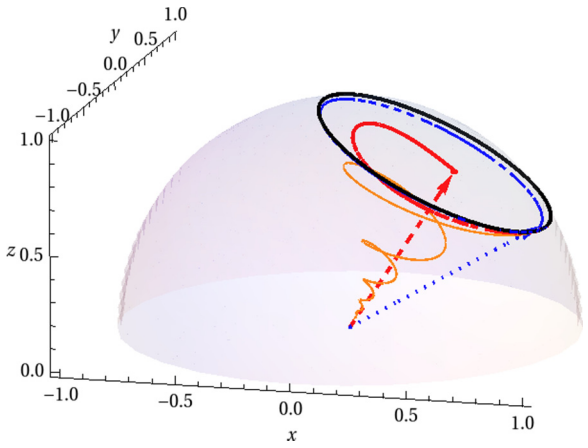

FIG. 1. (Color online) The evolution of the system can be illustrated by the path traversed by the vector **R** in the Bloch sphere. By solving the master equation it is possible to analyze the decoherence process by means of the change in the absolute value of **R**, which implies the loss of purity of the system, and also its change of $\hat{z}$ component. The black dotted line corresponds to the unitary evolution, i.e., when the qubit evolves isolated from the environment in a circle on the sphere surface. The orange trajectory, which approaches the center of the sphere, corresponds to the δ-correlated noise with $\gamma_0 = \gamma_1 = 0.03\Delta$. We can see that after a few numbers of periods, the system looses coherence completely and the final state is a totally mixed one. Red and blue trajectories correspond to different values of parameters α_0 and α_1 of the Gaussian-correlated noise models. The red curve shows a more decoherent behavior and corresponds to a low value of $\alpha_0 = \alpha_1 = 0.03\Delta$, while the blue line to higher values $\alpha_0 = \alpha_1 = 30\Delta$. We can see that the slower the decay of noise correlations, the greater the decoherence on the qubit in the weak coupling case $\gamma_0 = \gamma_1 = 0.03\Delta$. We have set $\Omega = 0.5\Delta$.

by the low-frequency noise, it is particularly destructive (though it is said that can be reduced by tuning the linear longitudinal qubit-noise coupling to zero [24]). A further relevant contribution is the electromagnetic noise of the control circuit, typically Ohmic at low frequencies.

Gaussian noise. An interesting way to model the fluctuations is through a Gaussian-correlated noise. We assume that the operator $\delta\hat{\omega}_i(t)$ is given by a random function $\delta\omega_i(t)$ with $\langle\delta\hat{\omega}_i(t)\rangle_{\mathcal{E}} = 0$ and its correlation between the values of $\delta\omega_i(t)$ at two different times is nonzero only for this time interval. Explicitly,

$$\langle\delta\hat{\omega}_i(t_1)\delta\hat{\omega}_i(t_2)\rangle_{\mathcal{E}} = \Phi_i(t_1 - t_2), \tag{16}$$

where $\Phi_i(t)$ is a function sharply peaked at $t = 0$ and vanishing for $t > \tau_c$ for a critical time scale τ_c. We have set $\Phi_i(t) = \gamma_i\mathcal{F}(\alpha_i, t)$ as defined in Eq. (15), where $\mathcal{F}$ is a Gaussian-like function of time. By setting the parameter α_i (α_0 for the longitudinal noise since it affects the coupling in the $\hat{z}$ axis and α_1 the transverse noise coupling in $\hat{x}$-) of the model, we can study the low- or high-frequency noise contribution to decoherence. Therefore, in this case, decoherence depends on the interplay of α_0 and α_1 and the value of the dissipation constants γ_0 and γ_1. For example, in Fig. 1 we present the trajectory of the Bloch vector during a cyclic (or quasicyclic) evolution. The black circle on the surface of the Bloch sphere is the evolution of the vector **R** in the unitary case, i.e., $\gamma_0 = 0 = \gamma_1$. Herein, we see that in absence of environment the qubit performs a closed trajectory in a period τ, acquiring the known GP, $\phi_G = \pi[1 - \cos(\vartheta)]$, with $\vartheta = \Delta/(\sqrt{\Delta^2 + \Omega^2})$. By considering different values for the parameters of our noise model, γ_i and α_i, we can evaluate how the distinct environments affect the system's dynamics. In Fig. 1, we also present the different trajectories of the Bloch vector **R** for a value of $\gamma_0 = 0.03\Delta$ and $\gamma_1 = 0.03\Delta$. As γ_i are related to the square of the coupling constant, these values for γ_i represent a significant environment within the weak coupling approximation. The blue dotted line is the trajectory of the Bloch vector when $\alpha_0 = 30\Delta$ and $\alpha_1 = 30\Delta$. This trajectory is very similar to the unitary one, which means that the environment has little influence on the systems' dynamics. The blue arrow line that starts in the center of the sphere and goes to the surface indicates the position of the Bloch sphere after one cycle $\tau = 2\pi/\tilde{\Omega}$, $\tilde{\Omega} = \Delta/\sqrt{\Delta^2 + \Omega^2}$. The red solid arrow line is the trajectory for a low value of $\alpha_0 = 0.03\Delta = \alpha_1$. This is what we shall call low-frequency noise. In this case, we can note that the trajectory differs substantially from the unitary one, meaning the system's dynamics is affected by the decoherence process. Qualitatively, decoherence can be thought of as the deviation of probabilities measurements from the ideal intended outcome. Therefore decoherence can be understood as fluctuations in the Bloch vector **R** induced by noise. Since decoherence rate depends on the state of the qubit, we will represent decoherence by the change of $|\mathbf{R}|$ in time, starting from $|\mathbf{R}| = 1$ for the initial pure state, and decreasing as long as the quantum state loses purity. The red dashed Bloch vector after a cycle is no longer on the surface of the sphere, as can be seen in Fig. 1. The module of the red dashed Bloch vector has been reduced 16% after one cycle with respect to the module of the unitary Bloch vector.

As a particular case, we can mention a noise correlation function given by a function $\mathcal{F} = \delta(s)$. If the general environment considered in this approach is a bath of harmonic oscillators with a δ-correlation function ($J(\omega) \sim \omega$), then we will be modeling an ohmic bath in the limit of finite temperature [12]. This assumption implies that the only coefficients in Eq. (11) which are constant and nonzero are $D_{zz} = \gamma_0 k_B T$ and $D_{xx} = \gamma_1 k_B T$. This model is commonly known as dephasing. This modeling of the environment is also included in Fig. 1 for $\gamma_0 = \gamma_1 = 0.03\Delta$ with an orange line. It is easy to see that the Bloch vectors decay to the center of the sphere, losing purity faster than in the Gaussian model. In the latter, due to the presence of more terms in the master equation, the Bloch vector does not decay to the center of the sphere [25].

In Fig. 2, we present a different scenario since the trajectories presented correspond to a very weak environment $\gamma_0 = \gamma_1 = 0.03\Delta$. Once again, the black solid line is the reference for the unitary case, while the blue line (almost coincident with the black) is for high-frequency ($\alpha_0 = \alpha_1 = 30\Delta$) and the red one for low-frequency noise ($\alpha_0 = \alpha_1 = 0.003\Delta$). Here, the Bloch vector for the low-frequency noise (red) is 5% reduced with respect to the unitary Bloch vector after one cycle τ.

Finally, we can comment on the $1/f$ noise mentioned above. This noise can be modeled by a bath composed of an infinite set of harmonic oscillators (similarly to what has

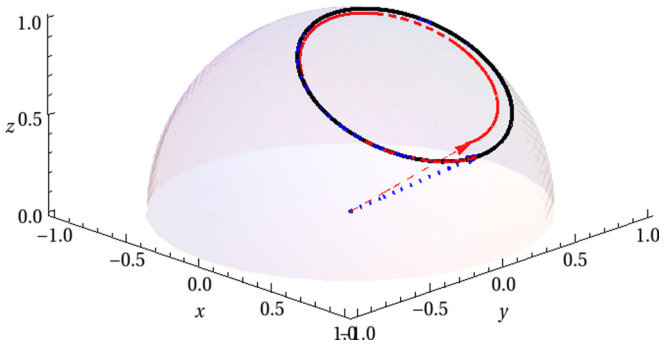

FIG. 2. (Color online) Numerical solution of the master equation for the trajectory of vector **R** in the Bloch sphere, for the Gaussian noise models for smaller dissipative constants $\gamma_0 = \gamma_1 = 0.03\Delta$. As before, the black solid line corresponds to the unitary evolution. The dotted red and blue trajectories correspond to different values of parameters α_0 and α_1 of the Gaussian-correlated noise models. The red curve shows a more decoherent behavior due to a low value of $\alpha_0 = \alpha_1 = 0.03\Delta$. The blue line corresponds to higher values $\alpha_0 = \alpha_1 = 30\Delta$. We have set $\Omega = 0.5\Delta$.

been done in the spin boson model [12]). At $T = 0$, the noise kernel $\nu(t)$ can be evaluated when $J(\omega) \sim A/\omega$. Then, the $1/f$ noise is determined by a correlation function $\nu(t) = -\gamma\Lambda\, CI(\Lambda t)$, where $CI(x)$ is the cosine integral function, and Λ is the typical infrared cutoff for the $1/f$ noise. In the high-temperature limit, this kernel is given by $\nu(t) = T\,\gamma\Lambda\,[-\pi/2\,t + \cos(\Lambda t)/\Lambda + t\,SI(\lambda t)]$, with $SI(x)$ the sine integral function. This quantitative modeling of the $1/f$ noise through a master equation approach is somewhat analogous to the effect of the phenomenological modeling of the noise through an ensemble of "spin fluctuators" [21]. In Fig. 3 we effectively note how harmful this type of noise is for the dynamics of the qubit, even in the very-low-temperature limit. Therein, the black solid line represents the unitary trajectory of the Bloch vector. In this model, the relevant parameter is the infrared frequency cutoff Λ. The blue dotted line is for a big value of the infrared cutoff $\Lambda = 0.1\Delta$, while the red solid line is for a low-frequency cutoff $\Lambda = 0.001\Delta$. Both cases are affected by decoherence. In the low-frequency cutoff case the module of the Bloch vector, indicated as a dashed red arrow from the center of the sphere, is reduced 20% in a cycle τ.

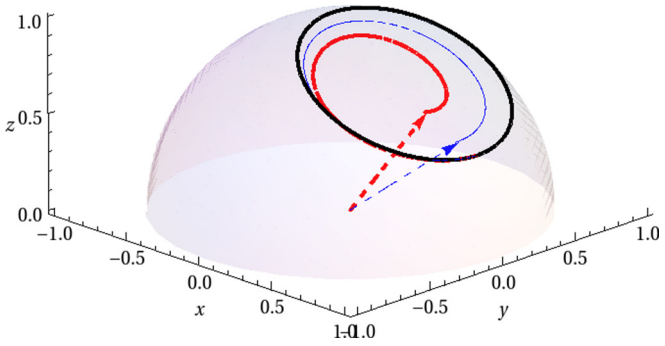

FIG. 3. (Color online) Numerical solution of the master equation for the trajectory of vector **R** in the Bloch sphere for the $1/f$ noise model. The black solid line indicates the trajectory of the qubit in absence of environment. The blue dotted line is the trajectory of the qubit under the influence of an environment with a "high" infrared cutoff $\Lambda = 0.1\Delta$. The red curve is the trajectory for a "low" infrared cutoff $\Lambda = 0.001\Delta$. We have set $\Omega = 0.5\Delta$.

III. APPLICATION: GEOMETRIC PHASE OF A SOLID-STATE QUBIT IN A NONUNITARY EVOLUTION

Practical implementations of quantum computing are always done in the presence of decoherence. Thus a proper generalization for the geometric phase to nonunitary evolutions is central in the evaluation of the robustness of geometric quantum computation. This generalization has been done in [10], where a functional representation of GP was proposed, after removing the dynamical phase from the total phase acquired by the system under a gauge transformation.

The GP for a mixed state under nonunitary evolution is then defined as

$$\Phi = \arg\left\{ \sum_k \sqrt{\varepsilon_k(0)\varepsilon_k(\tau)}\langle\Psi_k(0)|\Psi_k(\tau)\rangle e^{-\int_0^\tau dt\langle\Psi_k|\frac{\partial}{\partial t}|\Psi_k\rangle} \right\}, \tag{17}$$

where $\varepsilon_k(t)$ are the eigenvalues and $|\Psi_k\rangle$ the eigenstates of the reduced density matrix ρ, a solution of the master equation. In the last definition, τ denotes a time after the total system completes a cyclic evolution when it is isolated from the environment. Taking the effect of the environment into account, the system no longer undergoes a cyclic evolution. However, we will consider a quasicyclic path $\mathcal{P} : t\epsilon[0,\tau]$, with $\tau = 2\pi/\tilde{\Omega}$ [10]. It is worth noting that the phase in Eq. (17) is manifestly gauge invariant, since it only depends on the path in the state space, and that this expression, even though it is defined for nondegenerate mixed states, corresponds to the unitary geometric phase in the case that the state is pure (closed system).

It is expected that Berry's phase can be only observed in experiments carried out in a time scale slow enough to ignore nonadiabatic corrections but rapid enough to avoid destructive decoherence [13]. The noise-induced corrections to the GP depend on the value of parameters present in the noise model, for example, α_i and γ_i used in the above section. The purpose of this section is twofold: study how the GPs are affected by the different models of noise and explain some recent experimental setups where the GP has been measured in the presence of noise [17,18]. In the mentioned works, authors observed the Berry's phase in a superconducting qubit by different approaches. However, both experiments agree on the fact that the longitudinal noise affects the system's dynamics in a clearer way that the transversal noise. Another important fact is that in [18] the authors claimed to have observed the Berry phase under high-frequency fluctuations. They considered that this robustness of the GPs to high-frequency noise may be exploitable in the realization of logic quantum gates for quantum computation. Therefore we aim to explain these features of the GP for our model from a primary derivation of a master equation approach. In the following, we shall use the Gaussian model of noise for the study of the GP, since it is widely said that the $1/f$ can be reduced in spin-echo experiments by tuning the linear longitudinal qubit noise to

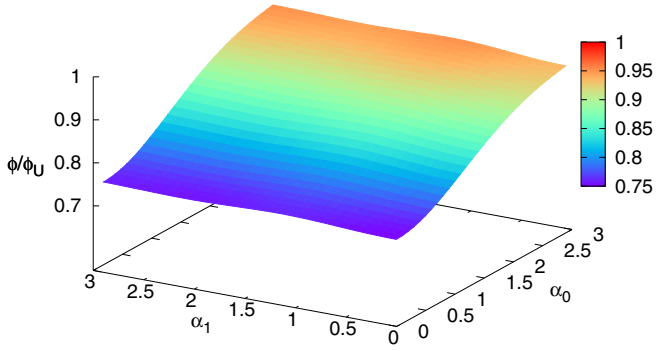

FIG. 4. (Color online) Ratio between the computed GP in the presence of noise and the one computed in the isolated case Φ_U, as a function of α_0 and α_1 (in units of Δ), with $\gamma_0 = \gamma_1 = 0.001\Delta$. The GP is more affected by the presence of longitudinal noise frequency α_0 since the rate is bigger. The GP does not considerably depend on the transversal noise α_1. We have set $\Omega = 0.5\Delta$.

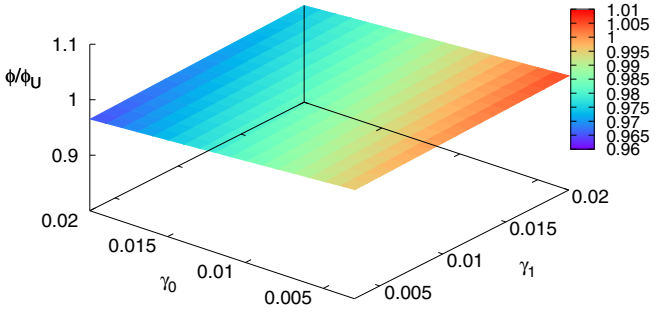

FIG. 6. (Color online) Rate between the computed GP in the presence of noise and the one computed in the isolated case Φ_U as a function of the dissipative constants γ_0 and γ_1 (in units of Δ), for a fixed value of $\alpha_0 = \alpha_1 = 10\Delta$. The correction to the GP is almost negligible for higher values of α_i, for weak coupling with the environment. We have set $\Omega = 0.5\Delta$.

zero [24]. In our Gaussian model, we have shown that the decoherence process was very dependent on the value of the α_i parameter, which we associated to a frequency. In all cases shown, decoherence was enhanced in the low-frequency case (small values of α, see Figs. 1 and 2).

In Fig. 4 we present the ratio between the GP Φ computed for a system evolving under a noisy environment after a cycle τ and the unitary one Φ_U, for different values of α_i, having γ_i fixed as $\gamma_0 = \gamma_1 = 0.001\Delta$. We show how this ratio varies once you have a fixed environment and a tunable frequency. Herein, we can note that the ratio does not practically change for different values of α_1, meaning that the transversal fluctuations are not relevant. However, we can see that the ratio varies considerably in the α_0 direction. The GP is visibly corrected for small values of α_0, i.e., for low-frequency noise in the longitudinal coupling of the qubit. This correction means that the Bloch vector has a relevant difference with the initial unitary Bloch vector since the environment induces more decoherence in the low-frequency case (see Fig. 1).

In Fig. 5 we again present the ratio between the GP Φ computed for a system evolving under a noisy environment

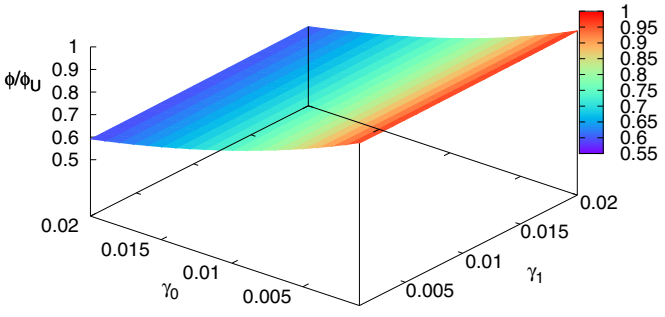

FIG. 5. (Color online) Rate between the computed GP Φ in the presence of noise and the one computed in the isolated case Φ_U as a function of the dissipative constants γ_0 and γ_1 (in units of Δ), for a fixed value of $\alpha_0 = \alpha_1 = 0.01\Delta$. The ratio is more affected by the longitudinal noise. We have set $\Omega = 0.5\Delta$.

after a cycle τ and the one unitary-computed Φ_U. This time we show how this ratio varies for different values of γ_0 and γ_1 for small values of α_i, say $\alpha_0 = \alpha_1 = 0.01\Delta$. It is easy to note that the GP Φ is very similar to the unitary GP Φ_U, in absence of longitudinal noise ($\gamma_0 = 0$), which means that the evolution is not considerably affected by the transverse noise. However, we can see a different behavior if we consider longitudinal noise ($\gamma_1 = 0$). The GP varies perceptibly as the environment coupled in the longitudinal direction is stronger (bigger values of γ_0). It is important to say that the relevant role of the tunable frequency α_i makes sense if we are dealing with a considerable environment which can effectively induce noise into our system's dynamics. For very small values of γ_0, Fig. 5 shows that the GP computed is similar to the unitary GP, independently of low- or high-frequency fluctuations.

In Fig. 6 we present the ratio between the GP Φ computed for a system evolving under a noisy environment after a cycle τ and the one unitary-computed Φ_U as a function of γ_0 and γ_1 for bigger values of α_i, say $\alpha_0 = \alpha_1 = 10\Delta$. Herein, we see that the system evolution in the presence of an environment with high-frequency fluctuations is very similar to the unitary evolution, since the GP acquired is practically similar to the Φ_U, for almost all values of γ_0. If we get a closer look, we can note that the difference between both phases becomes slow to increase for stronger values of γ_0. We believe that the situation depicted in Fig. 6 is very similar to the experimental situation reported in [18], where authors have measured the Berry phase for a superconducting qubit under high-frequency fluctuations.

Finally, in Fig. 7 we quantitatively show how the GP is affected by the longitudinal and transverse noises separately. We present the ratio between the observed GP Φ after a cycle τ and the unitary GP Φ_U as a function of both dissipative constants γ_i. We consider that the qubit is coupled to only one noise, i.e., that when we show how the ratio varies as a function of γ_0, the qubit is evolving only under a longitudinal noise and $\gamma_1 = 0$ (black-circled line). If the ratio varies as a function of γ_1, then the qubit is suffering the presence of transversal fluctuations only when $\gamma_0 = 0$ (blue-squared lines). We have also add the α_i parameter to have the full scenario. The correction to the GP is almost imperceptible to low-

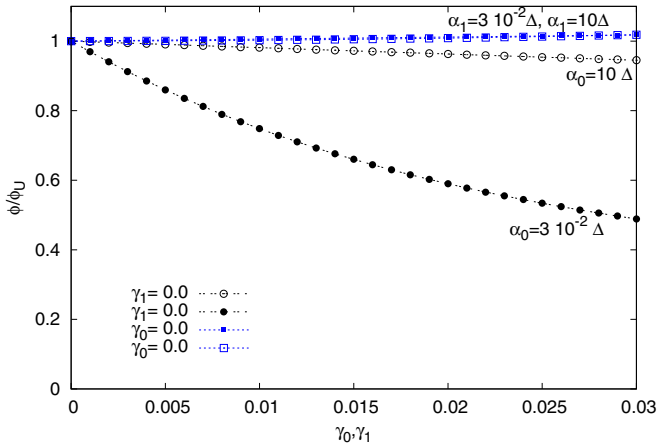

FIG. 7. (Color online) Ratio of the computed GP Φ in the presence of a noisy environment and the unitary GP Φ_U as a function of γ_0 and γ_1. The blue square–dotted line is the correction as a function of the transverse noise γ_1, for $\gamma_0 = 0$. The black circle–dotted line is the correction to the GP as a function of the longitudinal noise γ_0, when $\gamma_1 = 0$. Noise in the $\hat{z}$ direction corrects the phase more than noise in the transversal directions. These corrections are in agreement with the behavior of decoherence as a function of dissipative constants. All γ_i are measured in units of Δ.

and high-frequency transversal fluctuations (full and empty squares with $\alpha_1 = 0.03\Delta$ and $\alpha_1 = 10\Delta$, respectively), at least in the weak coupling limit. On the contrary, if the fluctuations of the environment are longitudinal, only those high-frequency ones do not considerably affect the measurement of the geometric phase. It is evident that low-frequency longitudinal noise induces a bigger correction to the phase (as can be seen from the full black-circled line with $\alpha_0 = 0.03\Delta$). These results agree with the previous analysis done on decoherence induced in the qubit and with the experimental setups reported of the observed geometric phase [17,18]. It is important to emphasize that our approach is general and allows several ways of modeling the environment coupled to the main system.

IV. FINAL REMARKS

We have considered the effective two-state Hamiltonian for the current-biased Josephson junction. The qubit has been shown to be fully manipulated with the control currents. Like any other quantum object, the qubit is subject to decoherence due to the interaction with uncontrolled degrees of freedom in its environment, including those in the device itself. These degrees of freedom appear as noise induced in the parameters entering the qubit Hamiltonian and also as noise in the control currents. These noise sources produce decoherence in the qubit, with noise, mainly, at microwave frequencies affecting the relative population between the ground and excited state, and noise or low-frequency fluctuations affecting the phase of the qubit. It is important to study the physical origins of decoherence by means of noise spectral densities and noise statistics.

We have derived a master equation for the two-level system including the combined effect of noise in the longitudinal and transversal directions. We considered different types of noise by defining their correlation function in time. We have mainly analyzed a Gaussian-like correlated type of noise, with low and fast decaying times that induce different decoherence processes in the low- or high-frequency parts of the environmental spectrum. We have even presented very correlated noise, where the noise kernel is proportional to a Dirac δ function in time and the $1/f$ known commonly used in spin fluctuator environments. For each type of noise presented, we numerically solved the master equation and obtained the system's dynamics. Qualitatively, decoherence can be thought of as the deviation of probability measurements from the ideal intended outcome. Therefore decoherence can be understood as fluctuations in the Bloch vector $\mathbf{R}$ induced by noise. Since decoherence rate depends on the state of the qubit, we have represented decoherence by the change of $|\mathbf{R}|$ in time, starting from $|\mathbf{R}| = 1$ for the initial pure state, and decreasing as long as the quantum state losses purity.

We have extended our analysis of decoherence to understand the corrections induced in the geometric phase, when the qubit evolves in time under fluctuations of the environment. Within the general picture of the master equation, we provide a framework to understand when the accumulated phase can still be found close to the unitary (Berry) one. We have focused on the effect of longitudinal and transverse noise on the global geometric phase. It is important to note that the relevant role of the tunable frequency α_i in our Gaussian model makes sense if we are dealing with a considerable environment which can effectively induce noise into our system's dynamics. For very small values of γ_0, we have shown that the GP computed is similar to the unitary GP, independently of low- or high-frequency fluctuations. We have also noted that the difference between both phases increases for stronger values of γ_0, becoming important when there are low-frequency longitudinal fluctuations in the environment. The differences among the phases are not considerable if the fluctuations of low frequency are originated in a transversal noise (γ_1). The correction to the GP is almost imperceptible to the transversal fluctuations, at least in the weak coupling limit.

It is important to recall that the results presented show that the system evolution in the presence of an environment with high-frequency fluctuations is very similar to the unitary evolution, since the GP acquired is practically similar to the Φ_U, for almost all values of γ_0. We believe that these results show a very similar scenario to that of the experimental situation reported in [18], where they have measured the Berry phase for a superconducting qubit under high-frequency fluctuations. In addition, we have checked that noise in the $\hat{z}$ direction induces a bigger correction to the phase than the noise in the transversal components. This correction agrees with the previous analysis done on decoherence induced in the qubit and with the experimental setups reported of the observed geometric phase. Comparison between theory and experiment verifies our understanding of the physics underlying the system as a dissipative two-level device. The analysis of the dephasing time scales may provide additional information about the statistical properties of the noise. Berry's phase measurements provide an important constraint to take into account regarding noise models and their correction induced over the GP, at least, at the times in which the experiments can be performed. The

comprehension of the decoherence and dissipative processes should allow their further suppression in future qubit designs or experimental setups.

ACKNOWLEDGMENTS

This work is supported by CONICET, UBA, and ANPCyT, Argentina.

[1] S. Pancharatnam, Proc. Indian Acad. Sci. A **44**, 247 (1956).
[2] M. V. Berry, Proc. R. Soc. London, Ser. A **392**, 45 (1984).
[3] J. A. Jones, V. Vedral, A. Ekert, and G. Castagnoli, Nature (London) **403**, 869 (2000).
[4] L. Faoro, J. Siewert, and R. Fazio, Phys. Rev. Lett. **90**, 028301 (2003).
[5] J. E. Sonier, Science **292**, 1695 (2001).
[6] P. Solinas, P. Zanardi, N. Zanghi, and F. Rossi, Phys. Rev. B **67**, 121307(R) (2003).
[7] P. Zanardi and M. Rasetti, Phys. Lett. A **264**, 94 (1999).
[8] Wang Xiang-Bin and M. Keiji, Phys. Rev. Lett. **87**, 097901 (2001).
[9] Erik Sjöqvist, D. M. Tong, L. Mauritz Andersson, Björn Hessmo, Markus Johansson, and Kuldip Singh, New J. Phys. **14**, 103035 (2012).
[10] D. M. Tong, E. Sjöqvist, L. C. Kwek, and C. H. Oh, Phys. Rev. Lett. **93**, 080405 (2004); **95**, 249902(E) (2005).
[11] A. Carollo, I. Fuentes-Guridi, M. F. Santos, and V. Vedral, Phys. Rev. Lett. **90**, 160402 (2003).
[12] F. C. Lombardo and P. I. Villar, Phys. Rev. A **74**, 042311 (2006).
[13] F. C. Lombardo and P. I. Villar, Int. J. Quantum Inf. **6**, 707713 (2008).
[14] Paula I. Villar, Phys. Lett. A **373**, 206 (2009).
[15] Fernando C. Lombardo and Paula I. Villar, Phys. Rev. A **87**, 032338 (2013).
[16] F. M. Cucchietti, J.-F. Zhang, F. C. Lombardo, P. I. Villar, and R. Laflamme, Phys. Rev. Lett. **105**, 240406 (2010).
[17] S. Berger, M. Pechal, A. A. Abdumalikov, Jr., C. Eichler, L. Steffen, A. Fedorov, A. Wallraff, and S. Filipp, Phys. Rev. A **87**, 060303 (2013).
[18] P. J. Leek, J. M. Fink, A. Blais, R. Bianchetti, M. Goppl, J. M. Gambetta, D. I. Schuster, L. Frunzio, R. J. Schoelkopf, A. Wallraff, Science **318**, 1889 (2007).
[19] Mahn- Soo Choi, J. Phys.: Condens. Matter **15**, 7823 (2003).
[20] J. M. Martinis, S. Nam, J. Aumentado, K. M. Lang, and C. Urbina, Phys. Rev. B **67**, 094510 (2003).
[21] E. Paladino, Y. M. Galperin, G. Falci, and B. L. Altshuler, arXiv:1304.7925 [cond-mat.mes-hall].
[22] Heinz-Peter Breuer and Francesco Petruccione, *The Theory of Open Quantum Systems* (Oxford University Publishing, Oxford, UK, 2007).
[23] J. P. Paz and W. H. Zurek, in *Environment Induced Superselection and the Transition from Quantum to Classical* in *Coherent Matter Waves, Les Houches Session LXXII*, edited by R. Kaiser, C. Westbrook, and F. David, EDP Sciences (Springer Verlag, Berlin, 2001), pp. 533–614; W. H. Zurek, Rev. Mod. Phys. **75**, 715 (2003).
[24] D. Vion, A. Aassime, A. Cottet, P. Joyez, H. Pothier, C. Urbina, D. Esteve, and M. H. Devoret, Science **296**, 886 (2002).
[25] G. Benenti, G. Casati, and G. Strini, *Principles of Quantum Computation and Information* (World Scientific, Singapore, 2004), Vol. 1.